Molecular Therapy
Original Article

Ancestral Adeno-Associated Virus Vector Delivery of Opsins to Spiral Ganglion Neurons: Implications for Optogenetic Cochlear Implants

Maria J. Duarte,[1,4] Vivek V. Kanumuri,[1,2,4] Lukas D. Landegger,[1] Osama Tarabichi,[1] Sumi Sinha,[1] Xiankai Meng,[1] Ariel Edward Hight,[1,3] Elliott D. Kozin,[1] Konstantina M. Stankovic,[1,2,3] M. Christian Brown,[1,2,3] and Daniel J. Lee[1,2,3]

[1]Eaton Peabody Laboratories, Massachusetts Eye and Ear, Harvard Medical School, Boston, MA, USA; [2]Department of Otology and Laryngology, Harvard Medical School, Boston, MA, USA; [3]Speech and Hearing Bioscience and Technology Program, Harvard Medical School, Boston, MA, USA

Optogenetics is a transformative technology based on light-sensitive microbial proteins, known as opsins, that enable precise modulation of neuronal activity with pulsed radiant energy. Optogenetics has been proposed as a means to improve auditory implant outcomes by reducing channel interaction and increasing electrode density, but the introduction of opsins into cochlear spiral ganglion neurons (SGNs) *in vivo* has been challenging. Here we test opsin delivery using a synthetically developed ancestral adeno-associated virus (AAV) vector called Anc80L65. Wild-type C57BL/6 mouse pups were injected via the round window of cochlea with Anc80L65 carrying opsin *Chronos* under the control of a CAG promoter. Following an incubation of 6–22 weeks, pulsed blue light was delivered to cochlear SGNs via a cochleosotomy approach and flexible optical fiber. Optically evoked auditory brainstem responses (oABRs) and multiunit activity in inferior colliculus (IC) were observed. Post-experiment cochlear histology demonstrated opsin expression in SGNs (mean = 74%), with an even distribution of opsin along the cochlear basal/apical gradient. This study is the first to describe robust SGN transduction, opsin expression, and optically evoked auditory electrophysiology in neonatal mice. Ultimately, this work may provide the basis for a new generation of cochlear implant based on light.

INTRODUCTION

The cochlear implant (CI) provides meaningful sound and speech perception to patients with severe to profound hearing loss by stimulating first-order auditory neurons called spiral ganglion neurons (SGNs).[1,2] Most CI users experience significant hearing improvement; however, outcomes vary widely across similar cohorts, and virtually all CI users report difficulty with background noise, listening in group environments, and music appreciation.[1,3,4] CI electrodes are arranged in a flexible linear array that approximates the tonotopic gradient of the cochlea, and modern devices have up to 22 platinum contacts for electrical stimulation of SGNs.[5] Notably, increasing the number of channels does not significantly improve spatial selectivity or audiologic performance.[6] These observations may be in part explained by longitudinal spread of electric current from individual electrodes, resulting in channel interaction and reduced spectral resolution.[7,8]

Optogenetics enables the precise modulation of cellular activity with optical stimulation following genetic manipulation of neurons to express microbial transmembrane proteins called opsins. Several studies have explored optogenetics as an alternative stimulus paradigm for auditory implants.[9–13] Unlike electricity, light can be focused to theoretically increase electrode density and reduce channel interaction. Optically evoked far-field potentials (e.g., optical auditory brainstem responses or oABRs) are observed during delivery of pulsed radiant light of appropriate wavelength to auditory neurons that express channelrhodopsin-2 (ChR2),[14,15] and laser collimation studies demonstrate spatial specificity in the cochlear nucleus (A.E. Hight et al., 2015, Assoc. Res. Otolaryngol., conference). New-generation opsins such as Chronos (Figure 1A) have superior on-off kinetics compared to the more commonly used ChR2, and they may be well suited to the auditory system that requires millisecond-level response times.[11]

To date, opsin expression of SGNs has been achieved using transgenic approaches or direct transduction via viral vectors (A.E. Hight et al., 2015, Assoc. Res. Otolaryngol., conference).[13,16] Vector delivery to target the peripheral or central auditory pathways *in vivo* requires invasive techniques (e.g., intra-uterine injections and craniotomies) (A.E. Hight et al., 2015, Assoc. Res. Otolaryngol., conference).[13,17] Transduction of SGNs has proven particularly challenging,[18,19] with expression of target proteins usually limited to a small number of neurons in mostly the basal turn of the cochlea.[20,21] A functional optogenetically driven CI would require high opsin expression levels along the cochlear axis if it is to provide an adequately broad auditory experience. A novel synthetic ancestral adeno-associated virus (AAV)

Received 8 January 2018; accepted 28 May 2018;
https://doi.org/10.1016/j.ymthe.2018.05.023.

[4]These authors contributed equally to this work.

Correspondence: Daniel J. Lee, MD, Massachusetts Eye and Ear, Harvard Medical School, 243 Charles Street, Boston, MA 02114, USA.
E-mail: daniel_lee@meei.harvard.edu

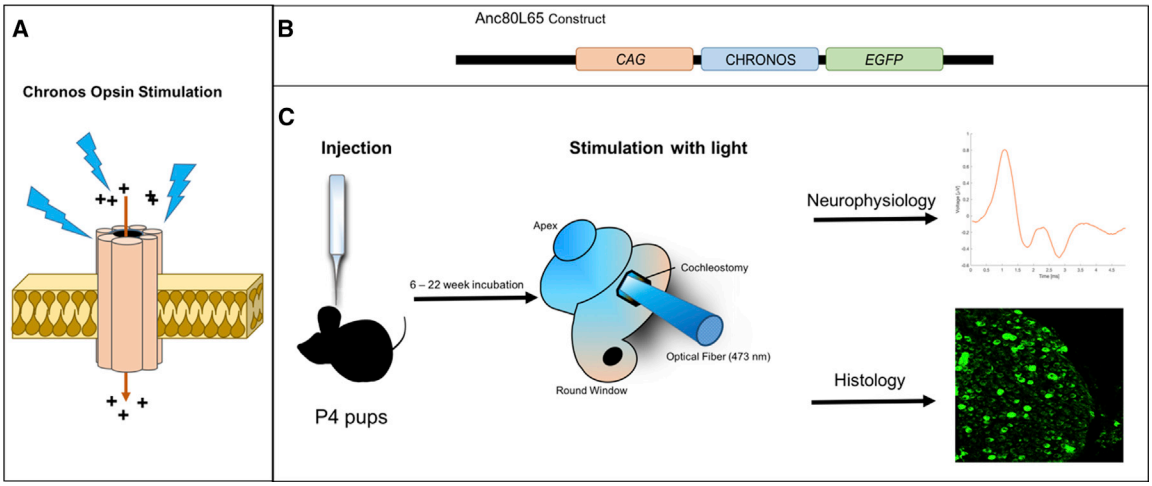

Figure 1. Methodology for Cochlear Optogenetics *In Vivo*

(A) Schematic showing Chronos, an excitatory opsin that forms a cation transmembrane channel. The channel opens in response to blue light (473 nm), allowing cation influx and depolarization of the neuron. (B) Schematic of the Anc80L65 viral vector, a gene addition construct, that includes an ITR-flanked expression cassette containing a CAG promoter sequence driving the transgene Chronos and an EGFP reporter gene, packaged in an Anc80L65 viral capsid. (C) Experimental sequence, showing P4 mice injected via the round window with vector (1 μL contains approximately 2.2×10^8 genome copies). Following an incubation period from 6 to 22 weeks, a cochleostomy was performed, and an optical fiber (diameter of 400 μm) was inserted into the proximal basal turn of the cochlea to deliver pulsed radiant energy at 473 nm. Neurophysiological responses were recorded during acute experiments of optical stimulation, and then the animal was sacrificed for confocal microscopy of cochlear sections.

vector (Anc80L65; Figure 1B) may provide a way forward.[22] Anc80L65 is an *in silico* reconstruction of an AAV, with capsid proteins that approach the ancestral state of AAV serotypes 1, 2, 3, 8, and 9.[22] Anc80L65 has higher transduction efficiency and stability compared to previous AAV vectors in a number of systems, including cochlear hair cells.[18,23–25] The Anc80L65 vector has not yet been coupled with optogenetic approaches, and its transduction efficiency has not been quantified in cochlear SGNs. Herein, we demonstrate successful viral-mediated expression and functionality of Chronos in post-mitotic SGNs using Anc80L65 in an *in vivo* murine model of cochlear optogenetics.

RESULTS

Robust Chronos Expression Was Observed in SGNs

Post-experiment histology confirmed Chronos-EGFP expression in cochlear SGNs in eight of nine mice. Co-localization of microtubule-associated protein 2 (MAP-2) and Chronos-EGFP in fluorescence microscopy revealed Chronos on SGN cell bodies (Figure 2) from base to apex of the cochlea (Figure 3). In mice with EGFP-positive neurons, a mean of 74% of SGNs expressed EGFP over the length of the cochlea. Expression of EGFP-Chronos was present in both the cytosol and cell membrane (Figure 4), and it appeared similar to prior work with Chronos and other opsins.[11,26] Some SGNs were completely saturated with EGFP signal (based on the cutoff saturation value on ImageJ software), averaging 31.5% in mice with opsin expression.

Apart from SGNs, we also observed opsin expression in organ of Corti hair cells; though this was not quantified, other inner ear studies focused on hair cells have demonstrated nearly 100% transduction of both inner and outer hair cells after round window injection of Anc80L65.[24] We also observed opsin expression in some supporting cells and in vestibular ganglion. Two control mice injected with saline (Figure 2D) and two wild-type non-injected mice (Figures 4A and 4B) demonstrated no EGFP expression in SGNs. Two control cochlea injected with empty vector (Anc80L65 carrying EGFP only; Figures 4C and 4D) demonstrated robust levels of EGFP expression on SGNs.

Optically Evoked Auditory Brainstem Responses

Following an incubation period of 6–22 weeks, stimulation of the cochlea with pulsed blue light was achieved using an optical fiber placed via cochleostomy (Figure 1C). Of nine mice injected with the Anc80L65-Chronos construct, eight were tested for neurophysiologic responses (one was sacrificed for histology without testing). Optically evoked auditory brainstem responses (oABRs; Figure 5A; 0- to 32-mW radiant energy and 28-Hz pulse rate) were observed in seven of the eight mice tested. No Chronos-EGFP expression was seen in the single mouse that failed to generate oABRs. In light-responsive mice, the oABR waveform consisted of 3–4 waveform peaks, although there was some variation in waveform morphology among subjects. Across animals, the mean oABR threshold was 9.4 mW. In general, latencies (1.2–4.0 ms) decreased and amplitudes (0.13–0.97 μV) increased with increasing radiant energy levels (Figures 5A and 5D). At 32 mW, the mean latency and amplitude were 1.9 ms and 0.65 μV, respectively. Both amplitude and latency were significantly correlated ($p < 0.0001$) with the percentage of SGNs expressing opsin.

In control experiments, oABRs were unchanged after facial nerve transection at the pes anserinus in one mouse (Figure 5F) and remained in spite of facial nerve transection (before testing) of 3 mice, suggesting that evoked potentials were not the result of

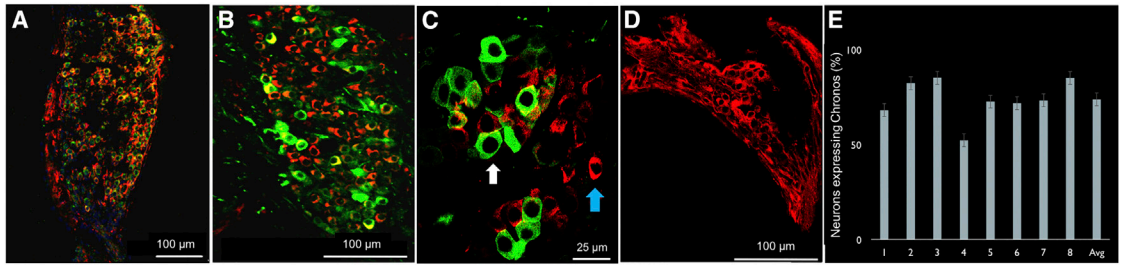

Figure 2. Cochlear Histology Demonstrating Robust Chronos-EGFP Expression in Spiral Ganglion Neurons following an 8-Week Incubation

Transverse sections were taken at the level of the middle turn of the cochlea. (A–C) Co-localization of Chronos-EGFP (green) and MAP-2 (red, a neuronal tubulin stain) in cell bodies of SGNs. (A) Low magnification confocal image of spiral ganglia demonstrate neurons (red) co-staining with Chronos-EGFP (green). (B) The same cochlea at higher magnification further demonstrates the pattern of co-localization. (C) High magnification image of the same cochlea shows individual neurons. White arrow points to a Chronos-EGFP-positive neuron (green label is strong so that it obscures the MAP-2 red label). Blue arrow points to a Chronos-EGFP-negative neuron. (D) Control cochlea showing MAP-2 staining after injection of saline with no Chronos-EGFP expression in neurons. (E) Percentage of SGN cells showing Chronos-EGFP expression in all mice injected with Anc-80L65 carrying Chronos opsin. Error bars represent SE. Percentage of expression per mouse significantly correlated ($p < 0.0001$) with both latency and amplitude of oABR response. Expression was not correlated with age of incubation. Scale bars, 100 μm (A, B, and D) and 25 μm (C).

stimulating non-auditory axons of passage (such as the intratemporal facial nerve). Acoustically evoked auditory brainstem response revealed normal thresholds in injected animals prior to cochleostomy (Figure 5E), indicating hearing preservation with vector injection and SGN transduction. There were no significant differences in oABRs or Chronos expression between mice with short (6-week) versus long (18-week) incubation times (Figure 6). Control mice (n = 2 saline injected, n = 2 empty Anc80L65 vector injected [Figure 5B], n = 2 non-injected wild-type) had no oABRs upon stimulation with light, despite having normal thresholds for acoustically evoked auditory brainstem responses.

Inferior Colliculus Responses

Multiunit activity in the inferior colliculus (IC) was measured using a penetrating recording probe placed along the IC isofrequency lamina. Robust IC activity during pulsed-light stimulation (Figures 7A, 7C, and 7D) was observed in all seven mice with oABRs. The mean threshold for IC responses was 6 mW (Figure 7D). There was broad activation along the different recording sites of the probe (Figure 7D), indicating activation of a broad range of characteristic frequencies that is consistent with the broad expression of Chronos from base to apex of the cochlea. Control mice that included those injected with saline (n = 2), empty vector (n = 2; Figure 5B), and non-injected mice (n = 2) had no IC responses to light stimulation of the cochlea. Finally, we observed that IC responses were synchronized during light stimulation rates of 28 pulses/s (Figure 7A) but less synchronized at higher rates. For pulse trains at 400 pulses/s, activity (measured as driven rate, or spikes/s) was significantly decreased and unsynchronized (Figure 7E). This was quantified by plotting the synchronization index (SI) as an average of three mice,[27] which fell from 0.86 at 28 Hz to 0.08 at 400 Hz (Figure 7F).

DISCUSSION

Efficient Delivery of Opsin to SGNs

Our study is the first to demonstrate efficient delivery of opsins to cochlear neurons in neonatal mice using the novel ancestral AAV vector Anc80L65. Overall, mice injected with the Anc80L65-Chronos construct demonstrated strong expression of Chronos (average 74% of SGN) that was relatively even along the cochlear basal/apical gradient (Figure 3). In these mice, light evoked oABRs and robust multiunit activity in the IC across the tonotopic axis (Figure 7). These functional responses are unprecedented in cochlear optogenetics to date.

Optogenetics and Synthetic AAV Vectors

In this study, we demonstrate the first use of Anc80L65 in combination with optogenetics in any neural system. In their original description of this novel vector, Vandenberghe and colleagues explored evolutionary intermediaries of commonly used AAVs in gene therapy, and they identified Anc80L65, a putative AAV ancestor with high stability, transduction efficiency, and low immunoreactivity.[22] Recent work has shown that this vector enables safe and robust gene delivery to the inner ear and recovery of hair cell function in models of deafness, enhancing its utility for cochlear optogenetics.[23,24] Our study is the first to demonstrate high-level gene transduction of SGNs using Anc80L65. SGNs are known to be refractory to efficient transduction via traditional AAV vectors.[19] Anc80L65-induced Chronos expression in SGNs *in vivo* was robust and durable for at least 18 weeks, with stable optically evoked potentials (Figure 6).

Previous work has demonstrated that Anc80L65 is a potent viral vector for the transduction of cochlear hair cells.[24,25] Interestingly, the level of SGN transduction achieved in our study (74%) exceeds what was observed in SGNs by Suzuki et al.[25] following direct injection of Anc80L65 in adult mice. There are several possible reasons for this difference: first, their technique employed a semicircular approach to the perilymphatic space of the cochlea. This is different from the round window approach we utilized, and it may be partially responsible for the disparate pattern of expression. In particular, a round window approach may be better suited to capturing the entire axis of the cochlea, since vectors tend to be most effective when injected as near as possible to target tissue. In addition, Suzuki et al.[25]

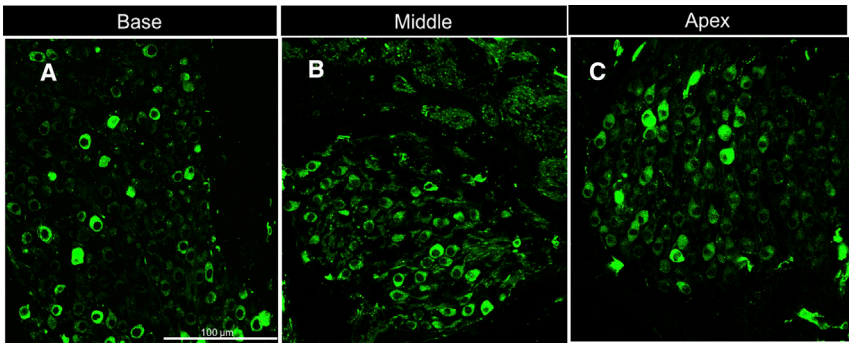

Figure 3. Cochlear Histology
(A–C) Cochlear histology demonstrating robust Chronos-EGFP expression in spiral ganglion neurons in the (A) base, (B) middle, and (C) apex. Scale bar, 100 μm for all three panels. Scale bar, 100 μm.

utilized a vector construct with a cytomegalovirus (CMV) promoter, whereas we utilized a CAG promoter that is more efficient than CMV in transducing many cell types, including neurons.[28,29] Finally, while we used neonatal mice, Suzuki et al.[25] injected adult mice. It is likely that a mature auditory system is more resistant to transduction, but the level of transduction achievable in adult mice via our method and our vector has yet to be elucidated.

Opsin expression of ChR2/CatCh in SGNs and optically evoked responses in hearing and deaf mice have previously been reported,[13] but they have required embryonic gene transfer and direct intra-uterine injection methods into the mouse oocyst.[13] This would be challenging to translate to clinical practice. Moreover, a strong baso-apical gradient in opsin expression was noted in SGNs following viral transduction with these vectors.[13] In contrast, we used a minimally invasive round window approach in neonatal mice that is analogous to procedures used in the clinic and operating room, including round window insertion of CI electrode arrays.[30] Trans-tympanic drug therapy is offered routinely for several inner ear pathologies (e.g., sudden sensorineural hearing loss and Meniere's disease), and direct round window injection is being widely explored as an avenue for drug delivery and gene therapy to the cochlea.[31] Transduction of SGNs has been explored using other AAV vectors[32] but has been limited by low efficiency.

Apart from the cochlea, studies that have paired different vectors with optogenetics in other organ systems, including the eye (retina and anterior segment) and hepatocytes, have yielded promising results.[22,30] Our findings thus have broad implications for the use of optogenetics beyond the inner ear (e.g., motor cortex and cardiac myocytes).[22,33–35]

Light-Evoked Responses from Cochlear Neurons Expressing Chronos

Light-evoked responses in our animals are almost certainly generated by Chronos-expressing SGNs, as there was no change in response after facial nerve transection, and control mice (as well as a mouse with negative histology) did not have responses. However, since opsin expression was also present in hair cells, they may have contributed to the optically induced responses. We view this contribution as small, since prior optogenetic work on hair cell transduction failed to evoke optical potentials.[36] Also, novel transgenic mice with ChR2 expression restricted to SGNs (developed by our group) have oABRs with similar waveform morphology as those observed here.[16] Additionally, if photosensitized hair cells had mediated responses, they may have produced an additional waveform component that preceded the major oABR response, as seen in acoustically driven auditory brainstem responses.[37,38]

Another unlikely generation source could be the optoacoustic effect.[39–42] While possible, we believe that this effect is unlikely to contribute to our responses because this effect is unlikely at wavelengths above infrared or near-infrared and because all of our control animals displayed absolutely no electrophysiology responses to optical stimulation (Figures 5B–5D and 7B). As such, the responses we observed likely originate primarily from optogenetic stimulation of transduced SGNs.

The opsin expressed in our mouse model, Chronos, has been shown to display among the fastest on-off kinetics of all currently available opsins.[11] Work in the cochlear nucleus by Hight et al.[11] has demonstrated that this opsin does extend the SI of collicular responses to optical stimulation over that found for ChR2. In our cochlear experiments, latency at maximal stimulation in our Chronos-expressing mice (1.9 ms) is shorter than prior work utilizing ChR2 (3.14 ms[13]) and closer to the average latency of 1.3 ms observed for acoustic stimuli.[43] These results suggest that, in a future optogenetic CI, Chronos could convey more of the fast transients found in the speech signal. For example, current clinical CI processors employing the spectral-peak (SPEAK) coding strategy use pulse rates of at least 250 pulses/s that are modulated by the speech signal.[44,45]

Limitations and Future Directions

There are several limitations to our animal model. First, opsin delivery was studied in the immature auditory system of young pups (postnatal day [P]4). Hearing onset in mice does not occur until P12, and prior work has demonstrated that the inner ears of neonatal mice are more responsive to vector-mediated delivery of genes, perhaps due to an immature immune system.[19,46] A translational model will also require successful transduction of post-mitotic SGNs in young adult and older mice. Prior work by our group transducing post-mitotic neurons in the cochlear nucleus with more traditional vectors,[12] as well as work done by other groups transducing adult mouse cochleae with Anc80L65,[25] is encouraging, though challenges will remain in adapting these techniques to our specific approach, vector construct, and optogenetics. A second limitation was that the present study used

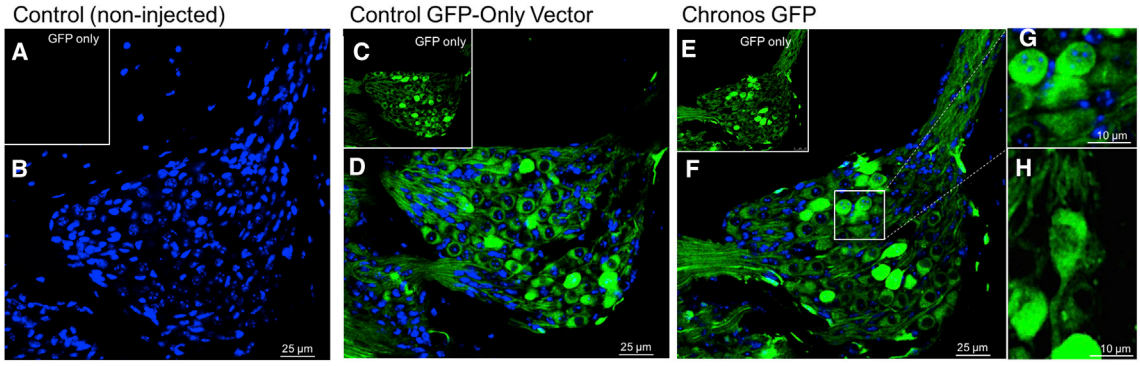

Figure 4. Cochlear Histology Comparing Spiral Ganglia at the Middle Turn of the Cochlea in Chronos-Expressing Neurons versus Controls
(A) Non-injected mice display no auto-fluorescence in the green channel. (B) For non-injected mice, an overlay of EGFP and DAPI images demonstrates only DAPI staining of neuronal nuclei. (C) Anc80L65 vector carrying EGFP only displayed high efficient transduction of spiral ganglion neurons, as seen in the green channel. (D) Overlay of EGFP and DAPI images. (E) Anc80L65 vector carrying Chronos demonstrated high transduction efficiency in a pattern very similar to the EGFP-only control. (F) Overlay of EGFP and DAPI images. (G) Enlarged image of neurons (outlined in F by white box) demonstrated cell membrane expression of Chronos. (H) Another neuron demonstrating cell membrane expression of Chronos in both the body and the axon. Overall, Chronos opsin was present in both the cell membrane and the cytosol of neurons. Scale bars, 25 μm (B, D, and F) and 10 μm (G and H).

hearing mice, but CIs are used in hearing-impaired individuals. While prior work with traditional AAV vectors has suggested that deafened cochleae may have better transduction rates,[19] full characterization of our approach on a deafened model will be needed to confirm this.

Finally, although our results suggest robust expression and low toxicity for several weeks to months post-injection, human gene therapy requires demonstration of stable expression on the order of years. The longest incubation in our cohort lasted 22 weeks and yielded negative oABRs and negative histology. This is likely due to a failed round window injection in this animal, since incubations of 18 weeks in other mice yielded robust histologic and functional responses, and Anc80L65 has been associated with stable expression of target genes for at least 6 months.[23] An additional concern in optogenetics is that long-term exposure to blue light has the potential to be toxic to the cochlea, though its effects on SGNs and supporting cells remain to be elucidated.[47,48] While we did not observe any evidence of light toxicity in our studies (electrophysiology responses remained the same despite repeated exposures to high-intensity blue light), this is an important consideration for chronic experimentation. The lower threshold and faster kinetics of Chronos compared to traditional opsins allows for reduced radiant light exposure that may decrease potential toxicity. Future work will examine any toxic effects of the light, and it will attempt to elucidate the minimum intensity of light required to achieve an adequate response. Hardware will aim to reduce both light intensity and time of exposure. Chronic studies that examine long-term durability and safety of Anc80L65-mediated opsin expression in the spiral ganglion will be the subject of future research.

Conclusions

Modern CIs are limited in spatial specificity due in part to channel interaction from electrical current spread. A CI based on light stimulation may reduce channel interaction and increase the number of independent channels of auditory information. Our study combines powerful optogenetic techniques, a minimally invasive approach, and a novel synthetic viral vector to demonstrate robust opsin delivery to the cochlear SGNs in neonatal mice. Ultimately, this work may provide the basis for novel CI technology based on light.

MATERIALS AND METHODS

Vector Preparation

A custom high-titer preparation of Anc80L65 vector construct was produced and purified via iodixanol sedimentation by the Gene Transfer Vector Core at the Schepens Eye Research Institute (http://vector.meei.harvard.edu) via previously described protocols.[22] Vector constructs contained an AAV inverted terminal repeat (ITR)-flanked expression cassette encoding CAG, a non-specific promoter containing the CMV early enhancer element, a portion of the chicken beta-actin gene, and a portion of the rabbit beta-globin gene, driving Chronos transgene as well as an EGFP reporter.

Animal Protocol

All experimental procedures were performed in accordance with institutional guidelines approved by the Massachusetts Eye and Ear Animal Care Committee (protocol 09-07-015).

Round Window Injections

Wild-type C57BL/6 mouse pups (Jackson Laboratory, Bar Harbor, ME) underwent round window injections at P4 (n = 10). Normal, neonatal mice were used in this study in order to pilot the feasibility of this new approach and to characterize the effects of transduction with this novel vector without confounders.

Injections were performed with a custom-made micropipette. The pipettes were pulled from capillary glass on a P-2000 pipette puller and beveled to a 20-μm diameter using a micropipette beveler. Pups were anesthetized by immersion in an ice bath for 3 min, and body

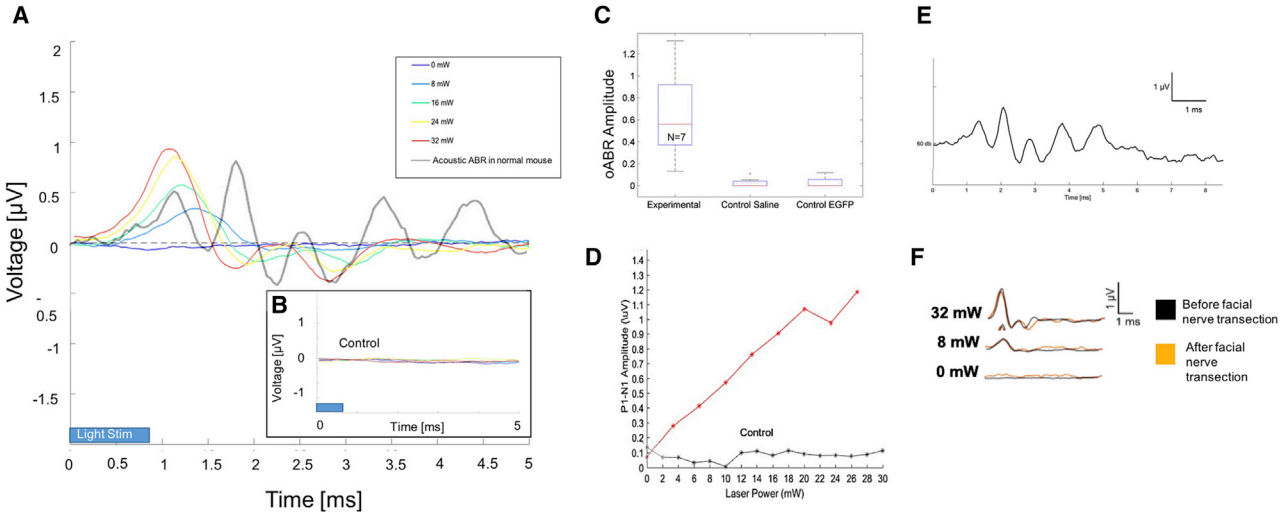

Figure 5. Optically Driven Auditory Brainstem Responses in Chronos-Positive Mice

(A) oABRs demonstrating multi-peaked waveform morphology. Response amplitude increased and latency decreased as a function of light power. (B) Control mouse injected with empty cassette vector (Anc80L65 coupled to GFP, but not carrying Chronos) displayed no oABR. (C) Average amplitudes of oABR at 32 mW power for mice injected with Anc80L65 vector carrying Chronos opsin, saline controls, and empty cassette controls. (D) Representative plot demonstrating level function for oABR amplitude as a function of optical power in one mouse with vector carrying Chronos opsin. (E) Acoustically evoked auditory brainstem responses (ABRs, 16 kHz pip tone stimulus) from one mouse demonstrating little effect following round window injection at P4. (F) oABRs before and after facial nerve transection, demonstrating little change in the response.

temperature was kept hypothermic throughout surgery via an ice-cooled platform. The left round window was exposed via a minimally invasive approach using a limited postauricular incision to expose the otic bulla. The round window niche was exposed and the tip of the micropipette was inserted through the round window membrane. A total of 1 μL ancestral AAV vector (Anc80L65) with Chronos opsin coupled to an EGFP marker was delivered slowly into the left inner ear perilymph (dose: 2.2×10^8 genome copies). Incisions were closed using a 6-0 black monofilament suture, and the pups were allowed to return to body temperature on a warming tray for 10 min before being returned to their mother. Control mice were injected with 1 μL saline using the same approach or with the following empty vector: 1 μL Anc80L65 coupled to EGFP, lacking Chronos. Non-injected mice were also used as controls.

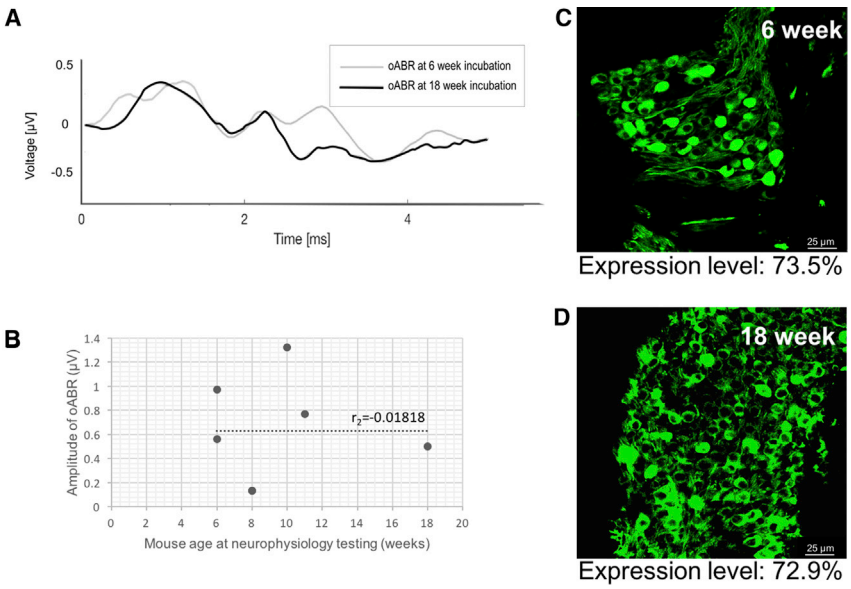

Figure 6. Varying Incubation Periods Yield Similar Opsin Expression and Electrophysiologic Responses

(A) oABRs measured at 6 or 18 weeks both displayed multi-peaked waveform morphology. (B) Scatterplot showing oABR amplitudes plotted against mouse age (in weeks). All subjects were injected as P4 pups. While amplitudes were variable, they were not associated with age (Spearman's rank correlation = −0.018). (C and D) Histology at 6 weeks (C) and 18 weeks (D) demonstrates similar opsin expression levels (73.5% versus 72.9%). Scale bar, 25 μm.

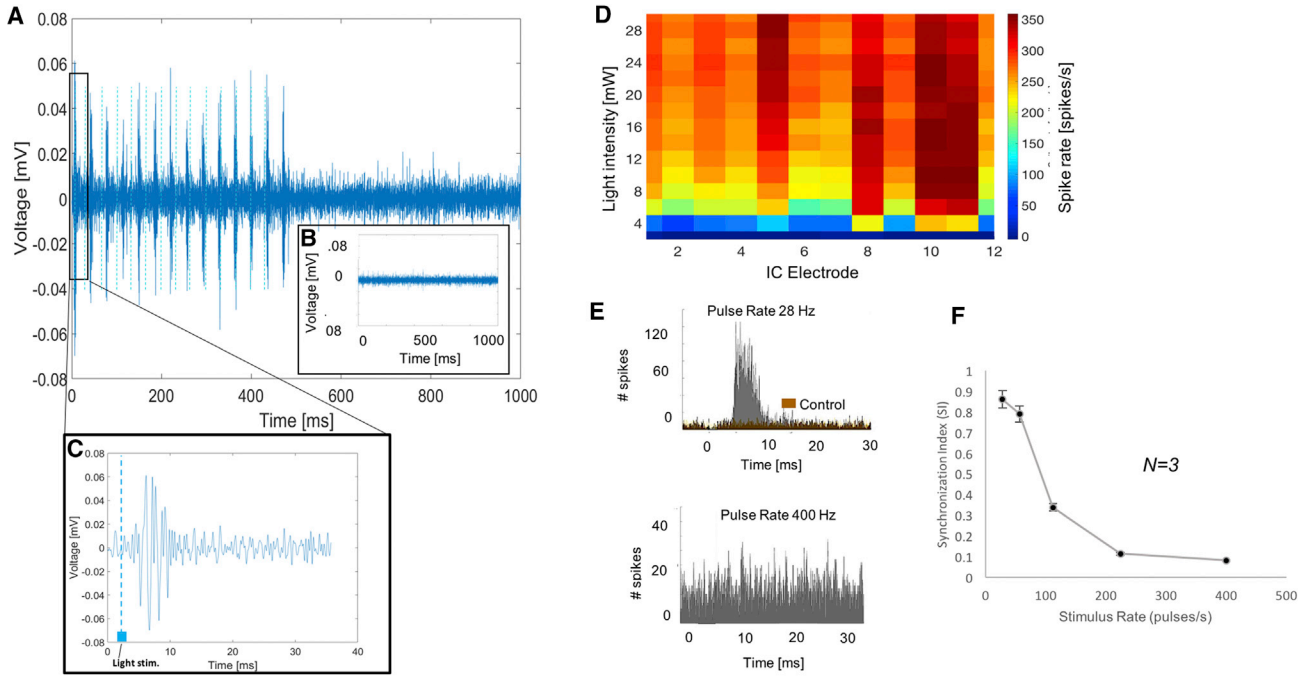

Figure 7. Optically Evoked Inferior Colliculus Responses in Chronos-Positive Mice

(A and C) Representative recording from one IC electrode demonstrates multiunit IC responses to light (14 light pulses in a train lasting 500 ms, with C showing response to a single pulse). (B) Control mouse injected with empty cassette Anc80L65 vector carrying only EGFP demonstrates no response to light. (D) Heatmap of spike rate in response to pulses of different light intensity (y axis), showing that spike rate increases above a threshold of about 6 mW. The pattern is even along the different IC recording electrodes (x axis), which are placed along the tonotopic axis of the IC (electrodes 1–3 are high characteristic frequency [CF] and electrodes 4–16 are middle and low CF, respectively). (E) Two post-stimulus time histograms showing number of spikes in a 20-ms period against time for all channels at two pulse rates. Top: Chronos-positive mouse response (gray histogram) to pulse rate (28 pulses/s) shows a synchronized peak in spikes at a latency of 6–8 ms. A control mouse (brown overlaid histogram) displayed only spontaneous IC activity. Bottom: response in same Chronos-positive mouse to 400 pulses/s shows loss of synchrony, though number of spikes is higher compared to controls. (F) Plot showing decrease in synchronization index (SI) as pulse rate increases (average of 3 mice). The SI is the magnitude of the vector of averaged spikes collected during the period between stimulus pulses. SI varies between 0 (no synchronization) and 1 (all spikes occurring exactly at the same phase of the stimulus period).[27]

Auditory Neurophysiology

Experiments were performed in a double-paneled, sound-attenuated chamber to avoid external stimuli. Following a 6- to 22-week incubation period (Figure 1C), mice were anesthetized with xylazine 20 mg/kg and ketamine 100 mg/kg via an intraperitoneal injection. Periodic boluses of additional ketamine 100 mg/kg were provided for additional anesthesia as needed. Following a minimal fur shave and 70% alcohol skin prep, a postauricular incision was performed and subcutaneous tissue was dissected. An anterior flap was then elevated until the pes anserinus of the facial nerve was identified. The tympanic bulla was identified immediately inferior to this. A microdrill was used to open the bulla and the cochlea was identified medially. A 500 μm cochleostomy was made anterior to the stapedial artery in the basal turn of the cochlea to enter the scala tympani. A 400 μm multimodal flexible optical fiber was introduced into the cochleostomy using a micromanipulator (Figure 1) to provide blue light (473 nm) from a 100 mW laser (Omicron Laserage, Germany). Light pulses were 1-ms pulses at a pulse rate of 28 pulses/s and with power ranging from 0 to 32 mW (average of 30 trials).

oABRs were recorded using needle electrodes placed subdermally near the pinna, the vertex, and on the back,[49] at varying light intensities, with 210–420 pulses averaged at each light intensity. Acoustic auditory brainstem responses were recorded in response 16-kHz tone pip stimuli (30 pips/s, averaged to a total of 512 pulses at each decibel [dB] level, 0–80 dB, with a step size of 10 dB). Latency was measured from the onset of light stimulus to the first oABR peak, and amplitude was measured as the difference from the top of the highest positive peak to the trough of the lowest negative peak.

Multiunit responses were measured in the IC via insertion of a 16 channel recording probe parallel to the IC isofrequency laminae. Light was delivered to the left cochlea in the manner above for 1-s trials (1 ms pulses, 14 pulses/train, 28–400 pulses/s; 0–32 mW in steps of 2.5 mW). The SI was calculated from IC recordings. The SI is defined as the magnitude of the vector of averaged spikes collected during the period between stimulus pulses; it varies between 0 (no synchronization) and 1 (all spikes occurring exactly at the same phase of the stimulus period). The SI would be 1 if all spikes occurred at

exactly the same phase of the stimulus period and 0 if they were evenly distributed over the period.[27]

Histologic Analysis

After oABR testing, mice were sacrificed with an overdose of ketamine (200 mg/kg) and transcardially perfused with 4% paraformaldehyde (PFA). The left cochlea was extracted and PFA was further flushed through the round window. The cochlea was post-fixed in PFA for 2 hr and then decalcified in EDTA for 5 days. It was then placed in sucrose and embedded for cryosectioning. Sections were 16 μm, and immunohistochemistry was used to stain for Chronos-EGFP and co-stained with MAP-2, a neuronal tubulin stain. Confocal microscopy was used to determine Chronos-EGFP expression (Figure 1). Confocal settings were determined by imaging non-injected control cochleae and adjusting the laser power and gain to eliminate all visible SGN autofluorescence. All images for injected cochleae were obtained utilizing those exact settings. Control images also underwent segmentation and thresholding via ImageJ software utilizing Otsu's algorithm. All non-control images were segmented for counting as well, and cells above the control threshold were considered to be expressing, while cells under the control threshold were considered to be auto-fluorescent and, thus, negative. Opsin expression was quantified manually using ImageJ software: fields displaying the spiral ganglion were chosen at random for each mouse, and cells were counted using the Cell Counter tool on ImageJ. Cells saturated with EGFP signal were defined as those cells flagged by the ImageJ system to be above the software's saturation cutoff value. Saturated cells were also counted within the same randomly selected fields as above. The same analysis was performed for control mice injected with saline and empty vector and for wild-type non-injected control mice.

AUTHOR CONTRIBUTIONS

M.J.D., V.V.K., L.D.L., S.S., X.M., and E.D.K. contributed to viral vector design, gene transfer, and histologic analysis. V.V.K., O.T., and A.E.H. performed all neurophysiological experiments. M.J.D., V.V.K., K.M.S., M.C.B., and D.J.L. designed and reported the experiments with topical input from all other authors.

ACKNOWLEDGMENTS

We would like to acknowledge the Vandenberghe group and the Schepens Eye Institute Gene Transfer Vector Core for help with plasmid amplification and vector creation, the Liberman lab for help with cochlear histology, Fadhel El May and Stephen McInturff for assistance with data analysis, and the MEEI Eaton Peabody Laboratories core staff for their support, specifically Evan Foss and Haobing Wang. This work was supported by NIDCD grants R01DC01089 (M.C.B.) and R01DC015824 (K.M.S.), DOD grant W81XWH-15-1-0472 (K.M.S.), the Bertarelli Foundation (D.J.L., M.C.B., and K.M.S.), the Nancy Sayles Day Foundation (K.M.S.), the Lauer Tinnitus Research Center (K.M.S.), a Marshall Plan Poster Series Fellowship (L.D.L.), and an NIH T32 training grant (V.V.K.).

REFERENCES

1. Vila, P.M., Hullar, T.E., Buchman, C.A., and Lieu, J.E. (2016). Analysis of Outcome Domains in Adult Cochlear Implantation: A Systematic Review. Otolaryngol. Head Neck Surg. *155*, 238–245.
2. Ganek, H., McConkey Robbins, A., and Niparko, J.K. (2012). Language outcomes after cochlear implantation. Otolaryngol. Clin. North Am. *45*, 173–185.
3. McDermott, H.J. (2004). Music perception with cochlear implants: a review. Trends Amplif. *8*, 49–82.
4. Vincenti, V., Bacciu, A., Guida, M., Marra, F., Bertoldi, B., Bacciu, S., and Pasanisi, E. (2014). Pediatric cochlear implantation: an update. Ital. J. Pediatr. *40*, 72.
5. Lenarz, T., Pau, H.-W., and Paasche, G. (2013). Cochlear implants. Curr. Pharm. Biotechnol. *14*, 112–123.
6. Friesen, L.M., Shannon, R.V., Baskent, D., and Wang, X. (2001). Speech recognition in noise as a function of the number of spectral channels: comparison of acoustic hearing and cochlear implants. J. Acoust. Soc. Am. *110*, 1150–1163.
7. Padilla, M., and Landsberger, D.M. (2016). Reduction in spread of excitation from current focusing at multiple cochlear locations in cochlear implant users. Hear. Res. *333*, 98–107.
8. Allitt, B.J., Harris, A.R., Morgan, S.J., Clark, G.M., and Paolini, A.G. (2016). Thin-film micro-electrode stimulation of the cochlea in rats exposed to aminoglycoside induced hearing loss. Hear. Res. *331*, 13–26.
9. Richardson, R.T., Thompson, A.C., Wise, A.K., and Needham, K. (2017). Challenges for the application of optical stimulation in the cochlea for the study and treatment of hearing loss. Expert Opin. Biol. Ther. *17*, 213–223.
10. Weiss, R.S., Voss, A., and Hemmert, W. (2016). Optogenetic stimulation of the cochlea-A review of mechanisms, measurements, and first models. Network *27*, 212–236.
11. Hight, A.E., Kozin, E.D., Darrow, K., Lehmann, A., Boyden, E., Brown, M.C., and Lee, D.J. (2015). Superior temporal resolution of Chronos versus channelrhodopsin-2 in an optogenetic model of the auditory brainstem implant. Hear. Res. *322*, 235–241.
12. Kozin, E.D., Darrow, K.N., Hight, A.E., Lehmann, A.E., Kaplan, A.B., Brown, M.C., and Lee, D.J. (2015). Direct visualization of the murine dorsal cochlear nucleus for optogenetic stimulation of the auditory pathway. J. Vis. Exp. (95), 52426.
13. Hernandez, V.H., Gehrt, A., Reuter, K., Jing, Z., Jeschke, M., Mendoza Schulz, A., Hoch, G., Bartels, M., Vogt, G., Garnham, C.W., et al. (2014). Optogenetic stimulation of the auditory pathway. J. Clin. Invest. *124*, 1114–1129.
14. Deisseroth, K. (2015). Optogenetics: 10 years of microbial opsins in neuroscience. Nat. Neurosci. *18*, 1213–1225.
15. Knöpfel, T., Lin, M.Z., Levskaya, A., Tian, L., Lin, J.Y., and Boyden, E.S. (2010). Toward the second generation of optogenetic tools. J. Neurosci. *30*, 14998–15004.
16. Meng, X., Hight, A.E., Kozin, E.D., Brown, C., Edge, A.S., and Lee, D.J. (2014). Generation of a Novel Transgenic ChR2 Mouse to Investigate Cochlear Implant Model Based on Optogenetics. Otolaryngol. Head Neck Surg. *151*, P86.
17. Darrow, K.N., Slama, M.C., Kozin, E.D., Owoc, M., Hancock, K., Kempfle, J., Edge, A., Lacour, S., Boyden, E., Polley, D., et al. (2015). Optogenetic stimulation of the cochlear nucleus using channelrhodopsin-2 evokes activity in the central auditory pathways. Brain Res. *1599*, 44–56.
18. Husseman, J., and Raphael, Y. (2009). Gene therapy in the inner ear using adenovirus vectors. Adv. Otorhinolaryngol. *66*, 37–51.
19. Kilpatrick, L.A., Li, Q., Yang, J., Goddard, J.C., Fekete, D.M., and Lang, H. (2011). Adeno-associated virus-mediated gene delivery into the scala media of the normal and deafened adult mouse ear. Gene Ther. *18*, 569–578.
20. Budenz, C.L., Wong, H.T., Swiderski, D.L., Shibata, S.B., Pfingst, B.E., and Raphael, Y. (2015). Differential effects of AAV.BDNF and AAV.Ntf3 in the deafened adult guinea pig ear. Sci. Rep. *5*, 8619.
21. Shu, Y., Tao, Y., Wang, Z., Tang, Y., Li, H., Dai, P., Gao, G., and Chen, Z.Y. (2016). Identification of Adeno-Associated Viral Vectors That Target Neonatal and Adult Mammalian Inner Ear Cell Subtypes. Hum. Gene Ther. *27*, 687–699.
22. Zinn, E., Pacouret, S., Khaychuk, V., Turunen, H.T., Carvalho, L.S., Andres-Mateos, E., Shah, S., Shelke, R., Maurer, A.C., Plovie, E., et al. (2015). In Silico Reconstruction

of the Viral Evolutionary Lineage Yields a Potent Gene Therapy Vector. Cell Rep. *12*, 1056–1068.

23. Pan, B., Askew, C., Galvin, A., Heman-Ackah, S., Asai, Y., Indzhykulian, A.A., Jodelka, F.M., Hastings, M.L., Lentz, J.J., Vandenberghe, L.H., et al. (2017). Gene therapy restores auditory and vestibular function in a mouse model of Usher syndrome type 1c. Nat. Biotechnol. *35*, 264–272.
24. Landegger, L.D., Pan, B., Askew, C., Wassmer, S.J., Gluck, S.D., Galvin, A., Taylor, R., Forge, A., Stankovic, K.M., Holt, J.R., and Vandenberghe, L.H. (2017). A synthetic AAV vector enables safe and efficient gene transfer to the mammalian inner ear. Nat. Biotechnol. *35*, 280–284.
25. Suzuki, J., Hashimoto, K., Xiao, R., Vandenberghe, L.H., and Liberman, M.C. (2017). Cochlear gene therapy with ancestral AAV in adult mice: complete transduction of inner hair cells without cochlear dysfunction. Sci. Rep. *7*, 45524.
26. Ronzitti, E., Conti, R., Zampini, V., Tanese, D., Foust, A.J., Klapoetke, N., Boyden, E.S., Papagiakoumou, E., and Emiliani, V. (2017). Submillisecond optogenetic control of neuronal firing with two-photon holographic photoactivation of Chronos. J. Neurosci. *37*, 10679–10689.
27. Dynes, S.B.C., and Delgutte, B. (1992). Phase-locking of auditory-nerve discharges to sinusoidal electric stimulation of the cochlea. Hear. Res. *58*, 79–90.
28. Niwa, H., Yamamura, K., and Miyazaki, J. (1991). Efficient selection for high-expression transfectants with a novel eukaryotic vector. Gene *108*, 193–199.
29. Lawlor, P.A., Bland, R.J., Mouravlev, A., Young, D., and During, M.J. (2009). Efficient gene delivery and selective transduction of glial cells in the mammalian brain by AAV serotypes isolated from nonhuman primates. Mol. Ther. *17*, 1692–1702.
30. Nordfalk, K.F., Rasmussen, K., Bunne, M., and Jablonski, G.E. (2016). Deep round window insertion versus standard approach in cochlear implant surgery. Eur. Arch. Otorhinolaryngol. *273*, 43–50.
31. Plontke, S.K., Hartsock, J.J., Gill, R.M., and Salt, A.N. (2016). Intracochlear Drug Injections through the Round Window Membrane: Measures to Improve Drug Retention. Audiol. Neurotol. *21*, 72–79.
32. Wise, A.K., Tu, T., Atkinson, P.J., Flynn, B.O., Sgro, B.E., Hume, C., O'Leary, S.J., Shepherd, R.K., and Richardson, R.T. (2011). The effect of deafness duration on neurotrophin gene therapy for spiral ganglion neuron protection. Hear. Res. *278*, 69–76.
33. Mathis, M.W., Mathis, A., and Uchida, N. (2017). Somatosensory Cortex Plays an Essential Role in Forelimb Motor Adaptation in Mice. Neuron *93*, 1493–1503.e6.
34. Weible, A.P., Piscopo, D.M., Rothbart, M.K., Posner, M.I., and Niell, C.M. (2017). Rhythmic brain stimulation reduces anxiety-related behavior in a mouse model based on meditation training. Proc. Natl. Acad. Sci. USA *114*, 2532–2537.
35. Wang, Y., Lin, W.K., Crawford, W., Ni, H., Bolton, E.L., Khan, H., Shanks, J., Bub, G., Wang, X., Paterson, D.J., et al. (2017). Optogenetic Control of Heart Rhythm by Selective Stimulation of Cardiomyocytes Derived from Pnmt^{+} Cells in Murine Heart. Sci. Rep. *7*, 40687.
36. Wu, T., Ramamoorthy, S., Wilson, T., Chen, F., Porsov, E., Subhash, H., Foster, S., Zhang, Y., Omelchenko, I., Bateschell, M., et al. (2016). Optogenetic Control of Mouse Outer Hair Cells. Biophys. J. *110*, 493–502.
37. Buran, B.N., Strenzke, N., Neef, A., Gundelfinger, E.D., Moser, T., and Liberman, M.C. (2010). Onset coding is degraded in auditory nerve fibers from mutant mice lacking synaptic ribbons. J. Neurosci. *30*, 7587–7597.
38. Yuan, Y., Shi, F., Yin, Y., Tong, M., Lang, H., Polley, D.B., Liberman, M.C., and Edge, A.S. (2014). Ouabain-induced cochlear nerve degeneration: synaptic loss and plasticity in a mouse model of auditory neuropathy. J. Assoc. Res. Otolaryngol. *15*, 31–43.
39. Verma, R.U., Guex, A.A., Hancock, K.E., Durakovic, N., McKay, C.M., Slama, M.C.C., Brown, M.C., and Lee, D.J. (2014). Auditory responses to electric and infrared neural stimulation of the rat cochlear nucleus. Hear. Res. *310*, 69–75.
40. Thompson, A.C., Fallon, J.B., Wise, A.K., Wade, S.A., Shepherd, R.K., and Stoddart, P.R. (2015). Infrared neural stimulation fails to evoke neural activity in the deaf guinea pig cochlea. Hear. Res. *324*, 46–53.
41. Teudt, I.U., Maier, H., Richter, C.P., and Kral, A. (2011). Acoustic events and "optophonic" cochlear responses induced by pulsed near-infrared laser. IEEE Trans. Biomed. Eng. *58*, 1648–1655.
42. Kallweit, N., Baumhoff, P., Krueger, A., Tinne, N., Kral, A., Ripken, T., and Maier, H. (2016). Optoacoustic effect is responsible for laser-induced cochlear responses. Sci. Rep. *6*, 28141.
43. Strenzke, N., Chanda, S., Kopp-Scheinpflug, C., Khimich, D., Reim, K., Bulankina, A.V., Neef, A., Wolf, F., Brose, N., Xu-Friedman, M.A., and Moser, T. (2009). Complexin-I is required for high-fidelity transmission at the endbulb of Held auditory synapse. J. Neurosci. *29*, 7991–8004.
44. Wilson, B., Lawson, D., and Zerbi, M. (1995). Advances in coding strategies for cochlear implants. Adv. Otolaryngol. Head Neck Surg. *9*, 105–129.
45. Xu, L., and Pfingst, B.E. (2008). Spectral and temporal cues for speech recognition: implications for auditory prostheses. Hear. Res. *242*, 132–140.
46. Iizuka, S., Sakurai, F., Shimizu, K., Ohashi, K., Nakamura, S., Tachibana, M., and Mizuguchi, H. (2015). Evaluation of transduction properties of an adenovirus vector in neonatal mice. BioMed Res. Int. *2015*, 685374.
47. Sparsa, A., Faucher, K., Sol, V., Durox, H., Boulinguez, S., Doffoel-Hantz, V., Calliste, C.A., Cook-Moreau, J., Krausz, P., Sturtz, F.G., et al. (2010). Blue light is phototoxic for B16F10 murine melanoma and bovine endothelial cell lines by direct cytocidal effect. Anticancer Res. *30*, 143–147.
48. Cheng, K.P., Kiernan, E.A., Eliceiri, K.W., Williams, J.C., and Watters, J.J. (2016). Blue Light Modulates Murine Microglial Gene Expression in the Absence of Optogenetic Protein Expression. Sci. Rep. *6*, 21172.
49. Akil, O., Oursler, A.E., Fan, K., and Lustig, L.R. (2016). Mouse Auditory Brainstem Response Testing. Bio Protoc. *6*, e1768.